ISSN 0869-5911, Petrology, 2019, Vol. 27, No. 6, pp. 553–566. © Pleiades Publishing, Ltd., 2019.
Russian Text © The Author(s), 2019, published in Petrologiya, 2019, Vol. 27, No. 6, pp. 601–616.

Experimental Study of the Peridotite–Basalt–Fluid System: Phase Relations at Subcritical and Supercritical *P-T* Conditions

N. S. Gorbachev[a], *, A. V. Kostyuk[a], A. N. Nekrasov[a], P. N. Gorbachev[a], and D. M. Sultanov[a]

[a] *Institute of Experimental Mineralogy, Russian Academy of Sciences, Chernogolovka, Moscow oblast, 142432 Russia*

**e-mail: gor@iem.ac.ru*

Received March 2, 2019; revised April 5, 2019; accepted April 19, 2019

Abstract—The paper reports experimental data on the partial melting of hydrous peridotite and basalt at pressures up to 4 GPa and temperatures up to 1400°C, as well as peridotite–basalt association in the presence of alkaline water–carbonate fluid as an experimental model of mantle reservoir with subducted oceanic protoliths. At partial melting of the hydrous peridotite at 3.7–4.0 GPa and 1000–1300°C, critical relations were observed over the entire studied pressure and temperature interval. At partial melting of hydrous basalt, critical relations between silicate melt and aqueous fluid were recorded at 1000°C and 3.7 GPa. The Na-alkaline silicate melt coexists with garnetite at 1100°C and with clinopyroxenite at 1150 and 1300°C. The peridotite–basalt–alkaline-aqueous–carbonate fluid at 4 GPa and 1400°C shows signs of critical relations between a carbonated silicate melt and a fluid. Reaction relations in the residual peridotite minerals with replacements of olivine ← orythopyroxene ← clinopyroxene ← potassic amphibole-type testify to a high chemical activity of the supercritical liquid. Experimental results suggest the existence of regions of partial melting (asthenospheric lenses) in the fluid-bearing upper mantle under supercritical conditions. These lenses contain near-solidus highly reactive supercritical liquids enriched in incompatible elements. Mantle reservoirs with supercritical liquids are geochemically similar to undepleted mantle and could serve as sources of magmas enriched in incompatible elements. The modal and cryptic upper mantle metasomatism under the effect of supercritical liquids leads to the refertilization of peridotite via enrichment of residual minerals in incompatible elements.

Keywords: mantle, peridotite, eclogite, fluid, experimental modeling, critical *P-T* parameters, metasomatism

DOI: 10.1134/S0869591119060031

INTRODUCTION

Geophysical and geochemical data indicate a large-scale crust–mantle exchange. Subduction of oceanic crust leads to the eclogitization of basalts and formation of fluid-rich subducted oceanic protoliths in a peridotite mantle (Taylor and Neal, 1989). Interest to studying the high-pressure fluid-bearing silicate systems is determined by the fluid effect on the phase composition and melting temperature of mantle, and the composition of generating silicate and salt (carbonate, chloride, and sulfide) melts. The extractive and transport properties of fluids at high pressure provide the mobilization and transfer of major and trace elements. Their interaction with mantle protolith is also responsible for mantle metasomatism.

An important feature of the fluid-bearing silicate systems is the critical relations between silicate melt and fluid at high pressures and temperatures, which are caused by their excellent mutual solubility. At critical parameters (P_cT_c), they show a complete miscibility with formation of a supercritical liquid. Above second critical point ($2P_cT_c$), *P-T* solidus of silicates is absent (Keppler and Audetat, 2005; Litasov and Ohtani, 2007). The existence of critical relations in the upper mantle and the composition of supercritical liquids are determined from inclusions in diamonds, from minerals in peridotite and eclogite xenoliths in kimberlites and alkali basalts, as well as in high-pressure peridotite and eclogite massifs emplaced in crust. Three major types of these fluids are distinguished: carbonate fluid enriched in Ca, Mg, Fe, salt fluid enriched in Na, K, H_2O, and Cl, and silicate fluid enriched in Si and Al (Klein-BenDavid et al., 2007; Navon et al., 1988; Weiss et al., 2009; Bogatikov et al., 2010). A complete miscibility between the salt and carbonate fluids, as well as between the carbonate and silicate end members of mantle fluids was confirmed experimentally. A complete miscibility between all three components is predicted in the diamond stability field (Wyllie and Ryabchikov, 2000; Kessel et al., 2005).

Critical relations have been experimentally studied in the simple water-bearing silicate systems of monomineral (quartz, nepheline, albite, and jadeite) and granite composition. In this series, the critical

parameters are within the intervals of 0.7–2.3 GPa and 550–1050°C, increasing in the same sequence.

The range of critical pressure decreases with addition of components, which increase the mutual solubility of melt and fluid, and increases with addition of fluid, which leads to the decrease of the mutual solubility of melt and fluid (e.g., CO_2) (Bureau and Keppler, 1999). The pressure of the second critical point is estimated at 12–13 GPa for the *Fo–En*–H_2O system, (Stalder et al., 2001), at 5–6 GPa for the eclogite–H_2O system (Kessel et al., 2005), 3.8 GPa for the peridotite–H_2O system (Mibe et al., 2007), and 3.8–4.0 GPa for the basalt–peridotite–H_2O system (Gorbachev, 2000). In the *Fo* + *En* + H_2O + CO_2 system, the $2P_cT_c$ parameters are estimated within 12–15 GPa (Wyllie and Ryabchikov, 2000).

In most of experimental works, the transition of a system in the supercritical state was determined in situ at superliquidus temperatures. A complete miscibility between silicate melt and fluid was observed visually during homogenization of melt–fluid association in anvil-with-hole apparatus (Bureau and Keppler, 1999) or using *X*-ray radiography (Mibe et al., 2007). Some works applied a quench method, when a transition from subcritical to supercritical state is identified from the composition of hydrous glass and fluid in frozen diamond traps (Kessel et al., 2005). However, these methods do not allow one to study in detail the phase composition of the transition from subcritical to supercritical state, as well as the interaction of supercritical liquids with residue. Moreover, most of the experiments were carried out at superliquidus temperatures. Taking into account the wide temperature interval between solidus and liquidus in mafic and ultramafic systems, as well as the formation of mantle magmas during partial melting of mantle, of great interest are studies of critical relations between melts and fluid in subliquidus region in the presence of residue. The structure and phase composition of experimental samples were taken as indicators of critical relations in such experiments (Gorbachev, 2000; Gorbachev et al., 2015). The composition of supercritical liquids and character of their interaction with silicate protolith depend on the relations of silicate and fluid components. The supercritical liquids could contain clusters typical of both melt and fluid (Wyllie and Ryabchikov, 2000). Such a dual nature of the supercritical liquids could affect the structure and phase composition of quench run products.

In order to obtain new data on phase relations in the upper mantle under supercritical conditions, the peridotite–H_2O and basalt–H_2O systems, as well as peridotite–basalt–$(Na, K)_2CO_3$–H_2O system have been studied experimentally at 3.7–4 GPa and 1000–1400°C. The studies of fluid-bearing eclogite and peridotite–eclogite systems as the experimental model of mantle reservoir with subducted oceanic protoliths are of interest for developing the petrogenetic models of suprasubduction magmatism.

EXPERIMENTAL PROCEDURE

Experiments were carried out at the Institute of Experimental Mineralogy of the Russian Academy of Sciences on an anvil-with-hole NL-40 apparatus using quench method. The study of the peridotite–H_2O and basalt–H_2O systems was carried out in hermetically welded Au capsules in a temperature range of 1000–1250°C, in an Au–Pd capsules at 1300°C, and in ferruginated Pt capsules at 1400°C. Quenching was conducted under isobaric conditions at switching the voltage. The peridotite–basalt–$(Na, K)_2CO_3$–H_2O system was studied using a multi-capsule technique with combined Pt-peridotite ampoule (Gorbachev, 1989). Starting material was loaded in a peridotite capsule manufactured by molding and sintering. This capsule, in turn, was placed in a platinum capsule, which then was hermetically welded.

Temperature was measured with a $Pt_{70}Rh_{30}/Pt_{94}Rh_6$ thermocouple. Pressure at high temperatures was calibrated using the quartz–coesite equilibrium curve. Temperature and pressure in the experiments were determined accurate to ± 5°C and ± 1 kbar (Litvin, 1991). The experiments lasted from 8 to 24 h.

After quenching, the capsules were cut into two parts along length, and each was pressed into polystyrene in a special mold under pressure and heating. Polished specimens were prepared from obtained tablets. The studies were carried out using a CamScan MV2300 electron microprobe equipped with YAG secondary and back-scattered electron detectors at the Institute of Experimental Mineralogy of the Russian Academy of Sciences, and a Link INCA Energy energy dispersive X-ray microanalyzer with Si(Li) detector at the Yaroslval Branch of the Physical and Technological Institute of the Russian Academy of Sciences.

EXPERIMENTAL RESULTS

Peridotite–H_2O System

Starting materials for experiments in the peridotite–H_2O system were garnet peridotite from xenoliths in the Obnazhennaya kimberlite pipe, Yakutia (collection by A. Ukhanov) and distilled water in a volumetric ratio of 0.4–0.6. The compositions of starting peridotite and coexisting phases in run products at 4 GPa and 1000–1300°C are listed in Table 1. Photos characterizing the structures and phase relations in the run products are shown in Figs. 1 and 2.

At 1000°C, the samples are characterized by a loose powdered structure formed by relicts of starting peridotite phases and the absence of intergranular silicate melt. Separate fragments of the sample resemble "breccia", in which oval olivine grains from 5 to 50 μm

Table 1. Representative chemical compositions of coexisting phases and starting peridotite in the peridotite–H_2O system at $P = 4.0$ GPa, $T = 1000$–1300°C

Phase	SiO_2	TiO_2	Al_2O_3	FeO	MnO	MgO	CaO	Na_2O	K_2O	Cr_2O_3	Total
$T = 1000$°C											
Ol	40.51	0.0	0.32	7.89	0.21	50.95	0.11	0.16	0.00	0.0	100.17
Grt	40.95	0.21	19.19	8.31	0.38	17.66	8.80	0.21	0.08	4.15	99.95
Cpx	52.04	0.18	3.19	1.71	0.17	16.45	21.51	1.28	0.04	0.56	97.11
Cht	0.46	0.25	18.63	16.62	0.0	13.45	0.43	0.23	0.07	44.81	94.95
$T = 1100$°C											
Ol	41.11	0.02	0.09	8.22	0.06	49.78	0.03	0.04	0.03	0.20	99.59
Grt	41.83	0.03	22.17	5.58	0.45	19.94	7.99	0.17	0.00	2.37	100.54
Cpx	52.77	0.15	2.57	2.55	0.17	18.56	21.52	0.05	0.05	0.70	99.10
Opx	54.64	0.0	3.70	5.23	0.29	34.52	0.83	0.23	0.00	0.32	99.76
Cht	0.71	0.17	37.38	10.41	0.56	19.37	0.13	0.12	0.03	34.40	103.28
$T = 1200$°C											
Ol	40.79	0.05	0.12	4.97	0.12	52.47	0.13	0.04	0.05	0.20	99.05
Cpx	50.06	0.18	5.33	5.56	0.26	16.05	18.28	0.01	0.00	0.52	96.31
K-*Amp*	49.62	2.71	13.86	9.80	0.25	4.50	13.77	1.24	1.36	0.00	97.61
Cht	0.08	0.00	4.23	9.57	0.44	15.43	0.16	0.27	0.00	68.10	98.37
Gl_{glob}	73.65	0.19	6.89	0.41	0.25	4.03	2.09	0.05	0.47	0.03	88.16
$T = 1300$°C											
Ol	41.52	0.14	0.09	5.66	0.04	54.90	0.08	0.00	0.00	0.01	102.67
Cpx	53.18	0.08	3.49	4.17	0.62	20.08	19.63	0.00	0.00	0.87	102.12
Opx	54.35	0.17	5.96	8.54	0.27	31.29	2.31	0.07	0.03	0.00	102.99
Starting peridotite											
Peridotite	42.84	0.04	1.74	7.19	0.13	40.52	3.39	0.12	0.03	0.56	97.57

in size (sometimes, up to 100 μm) are rimmed by Cr-bearing garnet (up to 4–5 wt % Cr_2O_3) and clinopyroxene (Fig. 1a). The "breccia" fragments are 100 μm in size. The samples contain accessory chromite. With temperature increase up to 1100°C, the structure and phase composition of the samples change insignificantly. The olivine and orthopyroxene relicts are surrounded by garnet–clinopyroxene aggregates. Garnet occurs only in the "breccia" matrix, and is absent among relict peridotite minerals. Clinopyroxene close in composition to diopside is present in matrix and as separate grains 10–20 μm in size.

However, at 1200 and 1300°C, the morphology and phase composition of the samples change after quenching. At 1200°C, garnet disappears, the characteristic brecciated structure is absent, but signs of reaction relations between olivine and clinopyorxene are preserved. Single oval olivine grains are overgrown by clinopyroxene and K-bearing amphibole (K-*Amp*) (Fig. 2). Silicate glass forms isolated microglobules. At 1300°C, the olivine coexists with clinopyroxene, which is replaced by orthopyroxene along rims.

The contents of trace elements in the coexisting phases are listed in Table 2. Figure 3 shows the primitive mantle-normalized trace element patterns for olivine, garnet, orthopyroxene, clinopyroxene as compared to these minerals from peridotite mantle xenoliths. The minerals from experimental samples at 1000 and 1100°C are characterized by the high contents of incompatible elements, which exceed their contents in olivine, garnet, orthopyroxene, and clinopyroxene from natural peridotite xenoliths. The REE, Ta, Nb, Zr, and Th contents in olivine are higher than those in garnet and pyroxenes at 1000°C and 1100°C, respectively. However, at 1200 and 1300°C, olivine shows no REE enrichment relative to pyroxene, while the REE content increases in the order of olivine < orthopyroxene < clinopyroxene.

Basalt–H_2O System

In the absence of aqueous fluid, the basaltic plagioclase + clinopyroxene assemblage changes subsequently into spinel-bearing assemblage at 8–10 kbar and eclogitic garnet + clinopyroxene assemblage with further pressure increase up to 15–18 kbar (Ringwood and Green, 1966). Kessel et al. (2005) studied the critical relations between a melt and a fluid in the eclog-

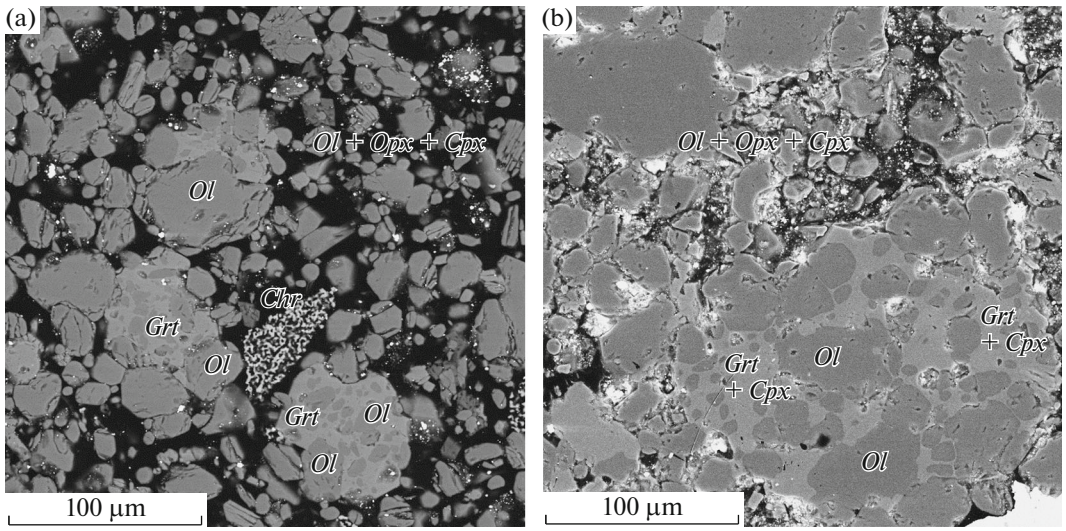

Fig. 1. BSE images of samples characterizing the structure and phase composition in the peridotite–H_2O system. (a) $T = 1000°C$. Disintegration of peridotite, quenched silicate glass is absent, isolated minerals and intergrowths of peridotite residue coexist with "reaction conglomerates", in which olivine relicts (*Ol*) are involved in a matrix of garnet composition (*Grt*). (b) $T = 1100°C$. Structure of "reaction conglomerate". Relicts of olivine (*Ol*) are overgrown by newly formed garnet–clinopyroxene (*Grt* + *Cpx*) aggregate. In photos, a "dark" matrix is polystyrene filling interstices between isolated peridotite residual minerals.

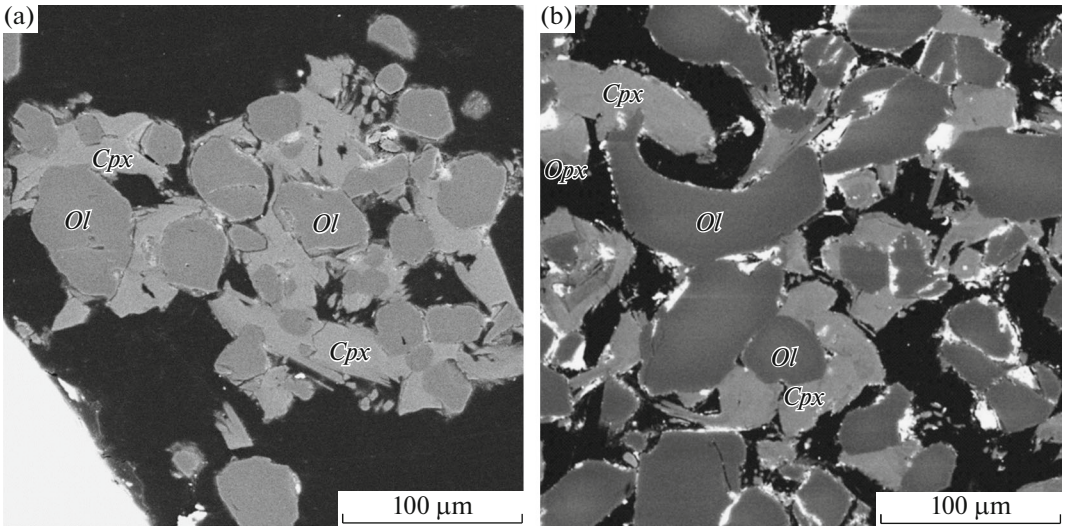

Fig. 2. BSE images of experimental samples characterizing the structure and phase relations of residue in the peridotite–H_2O system. (a) 1200°C; (b) 1300°C. In photos, a "dark" matrix is polystyrene. Figure 2a shows a wall of platinum capsule (upper left corner).

ite–H_2O system at 5–6 GPa. The transition from the subcritical to supracritical state was identified by the authors on the basis of composition of hydrous glass and fluid in frozen diamond traps. However, the change of phase composition during transition from subcritical to supercritical states and the interaction of supercritical liquids with residue have not been studied.

In our experiments, the tholeiite basalt–H_2O system was studied at 3.7–4.0 GPa and 1000–1300°C. The starting materials were powdered standard tholeiitic basalts CT-1, which is the chemical analogue of Siberian trap (collection by A. Almukhamedov), and distilled water in a volumetric ratio of 0.4–0.6. Microphotos of samples after experiments are given in Figs. 4–6, while the chemical compositions of coexisting phases are listed in Table 3.

At 1000°C, samples consisted mainly of garnet and clinopyroxene embedded in a matrix formed by a quench water-bearing silicate melt. The euhedral garnet crystals of grossular–pyrope composition up to

Table 2. Concentrations of trace elements (ppm) in the coexisting phases in the peridotite–H_2O system at $P = 4.0$ GPa, $T = 1000–1300$°C

Elements	$T = 1000$°C		$T = 1100$°C			$T = 1200$°C		$T = 1300$°C		
	Ol	*Grt*	*Ol*	*Cpx*	*Opx*	*Ol*	*Cpx*	*Ol*	*Cpx*	*Opx*
Li	0.38	0.82	0.61	1.02	1.96	0.79	4.16	0.68	1.44	1.54
Be	0.01	0.02	0.003	0.02	0.09	–	0.1	0.003	0.07	0.07
Ba	1.69	16.6	0.91	7.08	26.9	0.36	164.65	19.99	43.53	319.17
Th	2.92	1.08	0.04	0.37	0.69	0.01	0.94	0.02	0.45	0.5
U	1.86	0.67	0.1	0.23	0.38	0.03	0.35	0.1	1.22	0.72
Nb	35.43	15.86	1.21	2.44	6.86	0.69	9.89	1.6	3.51	3.49
Ta	0.93	0.39	0.38	0.08	0.18	0.02	0.23	0.01	0.15	0.17
La	3.3	2.72	0.18	1.49	3.02	0.02	5.66	0.09	7.78	6.92
Ce	16.25	9.71	1.1	4.55	4.78	0.02	10.89	0.07	12.74	15.39
Pb	0.29	0.82	0.08	0.26	0.91	0.25	1.02	0.98	2.22	1.48
Sr	4.44	32.67	2.27	46.5	19.28	1.07	228.67	2.45	57.36	90.96
Nd	24.02	12.37	3.02	2.3	2.18	0.01	4.17	0.01	6.68	7.45
Hf	0.78	0.31	0.91	0.16	0.19	–	0.34	0.01	0.25	0.41
Sm	6.44	2.72	1.75	0.53	0.57	0.02	0.77	0.07	1.5	2.02
Eu	1.43	0.61	0.57	0.18	0.17	0.004	0.96	0.11	0.56	0.5
Gd	8.93	4.41	3.37	1.45	1.3	0.01	2.62	0.01	4.32	4.54
Ti	1181.27	730.67	549.49	248.04	393.57	51.0	416.08	33.26	478.34	533.33
Dy	2.19	1.08	3.87	0.47	0.44	–	0.54	0.02	1	1.07
Y	9.49	4.3	26.03	2.87	2.35	0.05	3.82	0.07	6.32	6.41
Er	1.29	0.59	3.35	0.41	0.3	–	0.38	0.01	0.7	0.74
Yb	1.25	0.68	4.1	0.47	0.43	–	0.46	0.01	0.74	0.81
V	181.22	207.8	173	97.29	147.15	17.61	86.53	26.98	303.38	319.65
B	6.23	16.86	9.48	17.28	21.2	3.01	29.07	4.46	17.75	17.08
Zr	32.59	9.65	12.5	3.74	4.47	0.32	8.72	0.46	3.82	3.33

500 μm in size contain inclusions of relict clinopyroxene and ilmenite (Fig. 4a). The garnets are characterized by the elevated (up to 2.9 wt %) TiO_2 content, which indicates the presence of schorlomite end member ($Ca_3Ti_2(Si,Fe)_3O_{12}$) reaching > 10 mol %. Two structural types of clinopyroxene are distinguished: residual *Cpx*-1 observed as resorbed crystals and reaction *Cpx*-2 developed after garnet. Unlike the *Cpx-1*, the *Cpx*-2 is depleted in Na_2O and Al_2O_3, and has higher Mg/(Mg + Fe) = 0.78 against 0.63. Silicate melt is quenched as aggregates of micron-sized phases. The composition of quench products of melt (L_{Sil}-1) determined by defocused beam corresponds to trachyandesite. Silicate glasses at the contact of garnet with matrix (L_{Sil}-2) are characterized by the higher Na contents and have trachydacite composition (Fig. 4b).

At 1100°C, samples consist of single isolated clinopyroxene and garnet grains in a matrix consisting of silicate glass (Fig. 5a). Euhedral garnets up to 5 μm in size (*Grt*-1) are present as inclusions in clinopyroxenes and in rims of their crystals (*Grt*-2), as well as form numerous euhedral crystals or their intergrowths in a silicate matrix (*Grt*-3) (Fig. 5b). The pyrope–almandine–grossular garnet with Mg/(Mg + Fe) = 0.4 is characterized by low Cr_2O_3, but high TiO_2 (up to 2 wt %) and MnO (up to 0.65 wt %) contents. The clinopyroxene grains up to 100 μm are zoned (Fig. 5a). The inner zones of crystals (*Cpx*-1) with Mg# 0.6 have higher FeO, MgO, TiO_2, and MnO contents. The outer zones in contact with a silicate matrix (*Cpx*-2) are characterized by the higher CaO, Al_2O_3, Na_2O contents, and Mg/(Mg + Fe) = 0.7. The clinopyroxene contains garnet inclusions up to 5 μm in size. The matrix is represented by trachyandesite silicate glass filling interstices between clinopyroxene and garnet (Table 3).

At 1150 and 1300°C, the samples are characterized by massive structure and consist of clinopyroxene and K-bearing amphibole cemented by andesitic (at 1150°C) and trachyandesitic (at 1300°C) silicate glass (Fig. 6, Table 3).

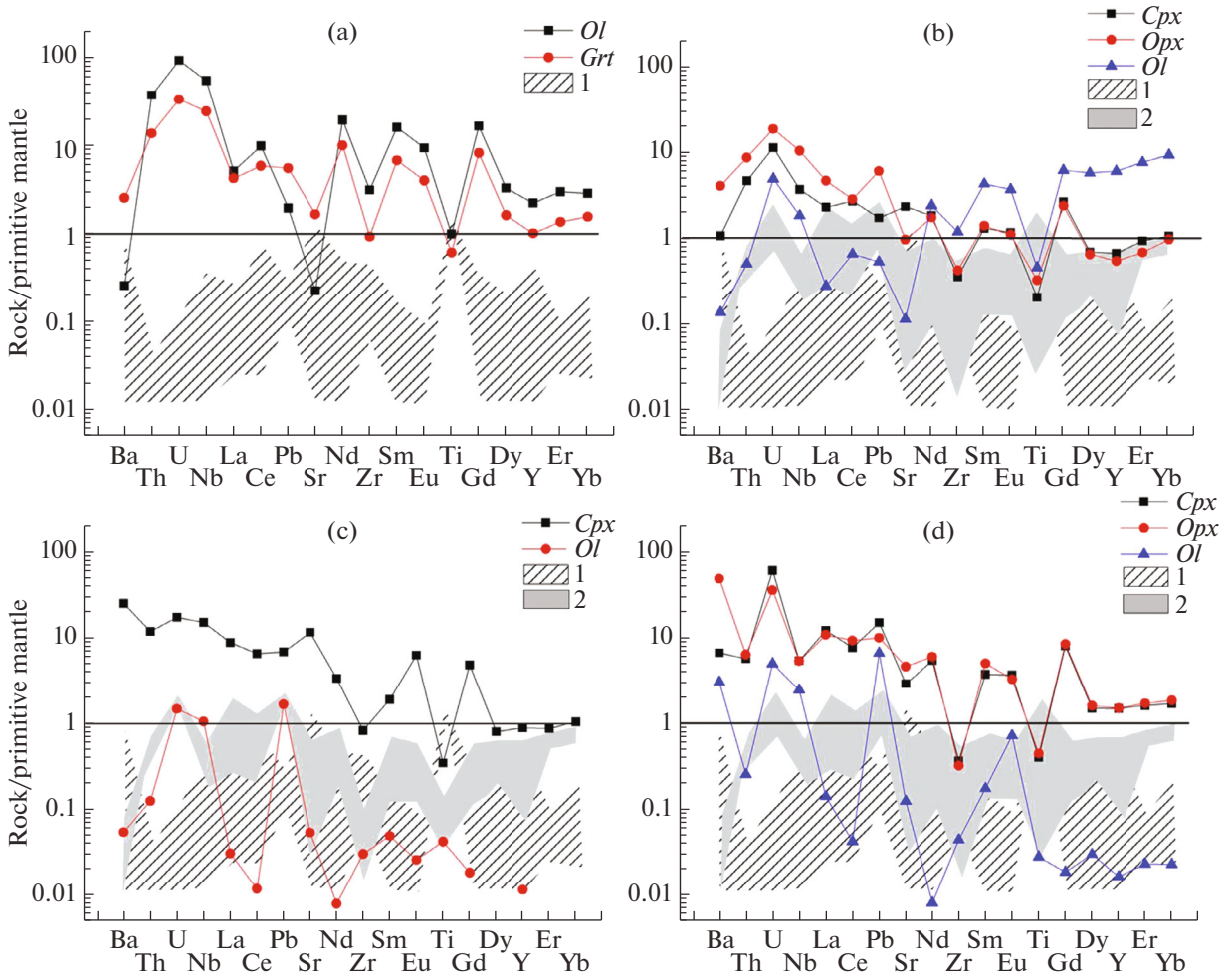

Fig. 3. Primitive mantle-normalized trace element contents in the olivine (*Ol*), garnet (*Grt*), orthopyroxene (*Opx*), and clinopyroxene (*Cpx*) of experimental samples at temperatures: (a) 1000°C, (b) 1100°C; (c) 1200°C; (d) 1300°C as compared to the olivine, clinopyroxene and orthopyroxene from mantle peridotite xenoliths (Gregoire et al., 2000): (1) olivine; (2) clinopyroxene + orthopyroxene.

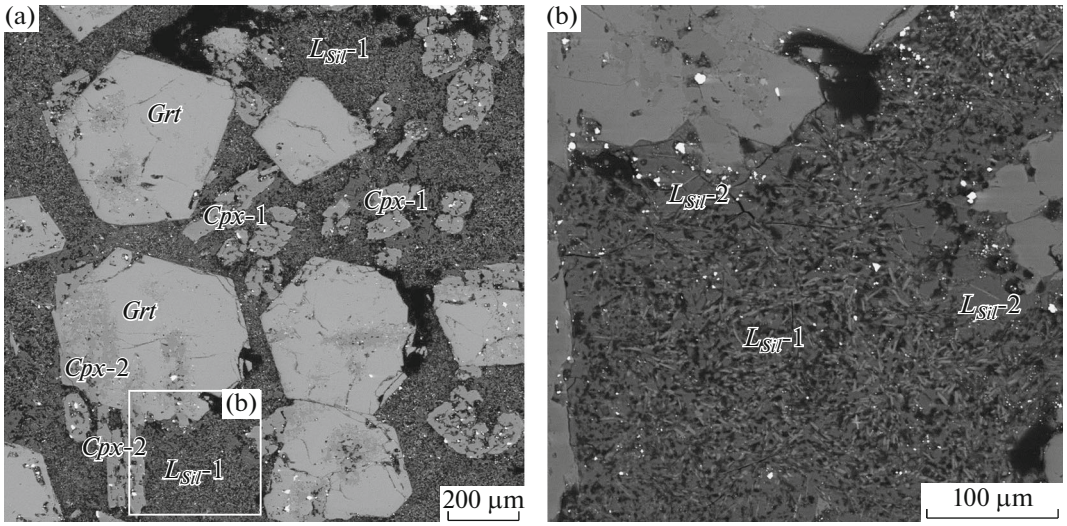

Fig. 4. BSE images of a sample characterizing phase composition during eclogitization of hydrous tholeiitic basalt and partial melting of eclogite under supercritical conditions. (a) Garnet crystals (*Grt*) with domains replaced by clinopyroxene (*Cpx*). Matrix is a quenched supercritical liquid (L_{Sil}-1). (b) Magnified part of the figure (a). Reaction melting of garnet with formation of glass rim (L_{Sil}-2). L_{Sil}-1 – quenched supercritical liquid. T = 1000°C, P = 3.7 GPa.

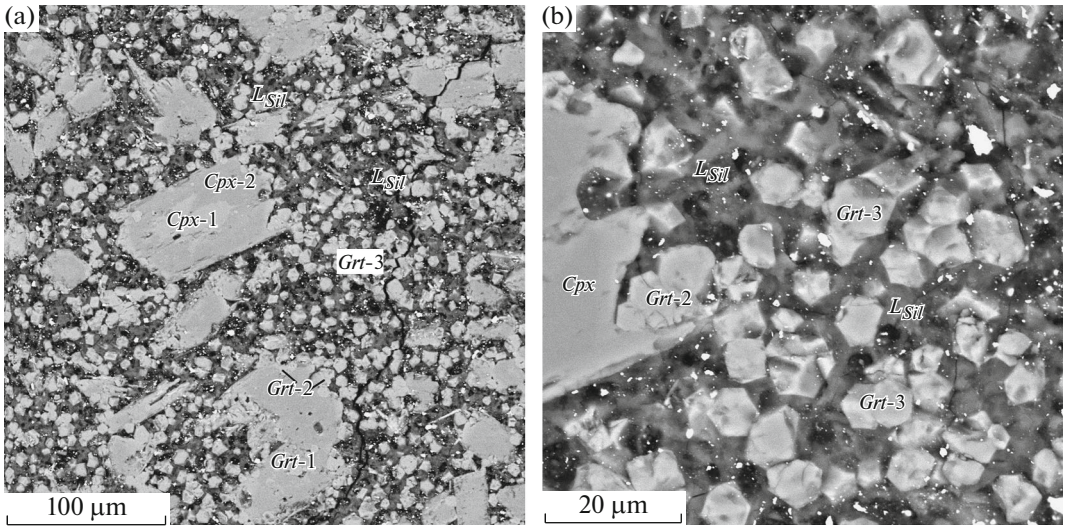

Fig. 5. BSE images of samples at eclogitization of hydrous tholeiitic basalt and partial melting of eclogite at 1100°C. (a) Zoned crystals of residual clinopyroxene (*Cpx*-1 and *Cpx*-2) and garnet (*Grt*-1 and *Grt*-2) in a matrix consisting of dispersed euhedral garnet crystals (*Grt*-3) or their intergrowths and silicate glass (L_{Sil}); (b) garnet crystals (*Grt*-3) or their intergrowths in a silicate matrix (L_{Sil}). Replacement of garnet (*Grt*-2) by clinopyroxene (*Cpx*).

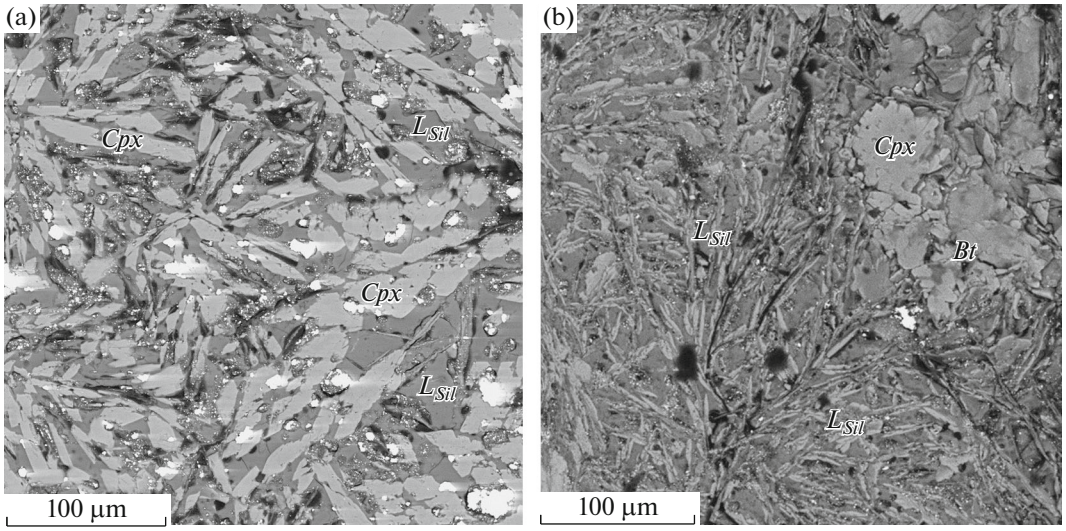

Fig. 6. BSE images of samples in the basalt–H_2O system. (a) 1150°C, residual clinopyroxene (*Cpx*) and K-amphibole are cemented by silicate glass (L_{Sil}); (b) 1300°C, relicts of clinopyroxene (*Cpx*) and biotite (*Bt*) in a glass (L_{Sil}) containing quenched phases.

Peridotite–Basalt–$(K, Na)_2CO_3$–H_2O System

In many works, the study of mantle–crustal interaction is based on the results of experiments in the volatile-free peridotite–basalt systems (Yaxley, 2000; Tumiati et al., 2013; Mallik and Dasgupta, 2012). Unlike these works, we used a multi-capsule technique with Pt-peridotite capsule and water–carbonate fluid. The peridotite capsule for experiments at 1400°C and 4 GPa was prepared from garnet peridotite described above. It was filled with a powdered mixture of tholeiite basalt CT-1 (~80 wt %), Na_2CO_3 and K_2CO_3 (of analytical grade) (~10 wt %), pyrrhotite (~ 10 wt %), and distilled H_2O (~20 wt % relative to silicate). Microphotos of the samples after experiments are shown in Fig. 7, while the chemical compositions of the coexisting phases are shown in Table 4.

Three zones are observed in the transverse section of the samples after experiment (Fig. 7a): zone of disintegrated peridotite capsule (Fig. 7c), reaction zone at the peridotite–basalt boundary, and basaltic zone (Fig. 7b) formed by quenching of supercritical fluid–melt. The basaltic zone consists of fine-grained (up to

Table 3. Representative composition of coexisting phases at melting of the basalt–H_2O system at $P = 3.7–4.0$ GPa, $T = 1000–1300°C$

Phase	SiO_2	TiO_2	Al_2O_3	Cr_2O_3	FeO	MnO	MgO	CaO	Na_2O	K_2O	Total
					$T = 1000°C$						
Grt	37.87	2.89	19.76	0.00	22.96	0.71	6.61	10.38	0.30	0.00	101.48
Cpx-1	52.25	0.33	3.59	0.04	10.34	0.32	12.47	18.95	1.41	0.00	99.72
Cpx-2	51.39	0.55	5.09	0.02	9.48	0.17	11.67	19.80	1.63	0.08	99.88
L_{Sil}-1	58.31	0.19	12.91	0.00	0.62	0.03	0.21	1.81	4.94	1.28	80.30
L_{Sil}-2	63.14	0.38	15.50	0.00	0.28	0.07	0.19	2.59	5.94	1.45	89.60
Ilm	4.90	46.92	3.23	0.00	38.77	0.38	3.06	1.72	0.17	0.08	99.24
					$T = 1100°C$						
Grt-1	38.39	1.02	21.37	0.22	19.30	0.48	7.88	10.36	0.02	0.00	99.04
Grt-2	38.90	1.10	20.59	0.04	19.59	0.65	7.88	10.69	0.21	0.01	99.70
Grt-3	38.40	1.18	21.39	0.05	20.21	0.48	7.78	10.81	0.15	0.02	100.47
Cpx-1	51.20	0.79	1.91	0.00	13.77	0.26	13.33	18.49	0.24	0.00	99.99
Cpx-2	52.76	0.53	4.78	0.13	7.74	0.16	12.42	19.32	1.82	0.00	99.74
L_{Sil}	60.03	1.33	15.88	0.00	1.67	0.05	0.20	3.35	4.89	0.77	88.18
					$T = 1150°C$						
Cpx-1	45.06	2.72	11.42	0.00	12.11	0.07	8.54	18.05	0.92	0.09	98.99
K-*Amp*	42.18	2.52	13.09	0.04	15.18	0.21	9.65	10.22	2.62	0.93	96.66
L_{Sil}	61.02	0.13	15.9	0.00	0.41	0.00	0.06	4.93	3.68	1.43	87.56
					$T = 1300°C$						
Cpx	49.18	2.43	13.87	0.11	7.13	0.02	8.95	19.83	2.30	0.37	104.19
Bt	45.87	2.53	13.28	0.00	7.43	0.20	17.00	8.77	1.09	4.67	100.84
L_{Sil}	60.15	0.29	17.72	0.02	0.46	0.00	0.00	1.97	5.60	2.69	88.90
					Transitional zone $T = 900°C$, $P = 12$ GPa (Okamoto and Maruyama, 2004)						
Grt	41.2	1.8	18.4	0.00	16.6	0.00	7.9	14.0	0.5	0.01	100.41
Cpx	56.4	0.76	13.1	0.00	5.12	0.00	7.6	10.1	6.2	0.06	99.34

Table 4. Compositions of the coexisting phases at partial melting in the peridotite–basalt-$(Na, K)_2CO_3$–H_2O system at $T = 1400°C$, $P = 4$ GPa

Phase	SiO_2	TiO_2	Al_2O_3	Cr_2O_3	FeO	MnO	MgO	CaO	Na_2O	K_2O	Total
Ol	40.23	0.40	0.78	2.36	6.08	0.12	50.20	0.18	0.38	0.04	100.58
K-*Amp*	41.78	0.85	15.02	0.10	6.56	0.21	14.36	10.87	2.09	1.50	93.37
Cpx	45.82	2.04	11.54	0.18	3.77	0.00	11.97	21.69	0.89	0.10	98.16
Opx	54.29	0.28	4.88	1.03	3.54	0.13	33.33	1.69	0.00	0.00	99.17
Phl	40.67	0.35	14.20	0.37	2.89	0.20	21.92	0.06	1.31	6.65	88.89
L_{Sil}-*Gl*	53.08	0.24	18.60	0.04	0.10	0.12	0.00	0.22	6.81	2.83	82.17
L_{Cb}	2.59	0.17	0.72	0.05	0.88	0.48	3.21	42.89	0.89	0.10	52.07

5 μm) silicate and carbonate aggregates, sulfide and aluminosilicate microglobules. Unlike subcritical conditions, no silicate glass is formed in the peridotite capsule under these conditions. The peridotite part of the sample consists of the isolated relicts and the intergrowths of olivine, orthopyroxene, and clinopyroxene. The residual minerals show reaction relations with the newly formed minerals in sequence orthopyroxene ←

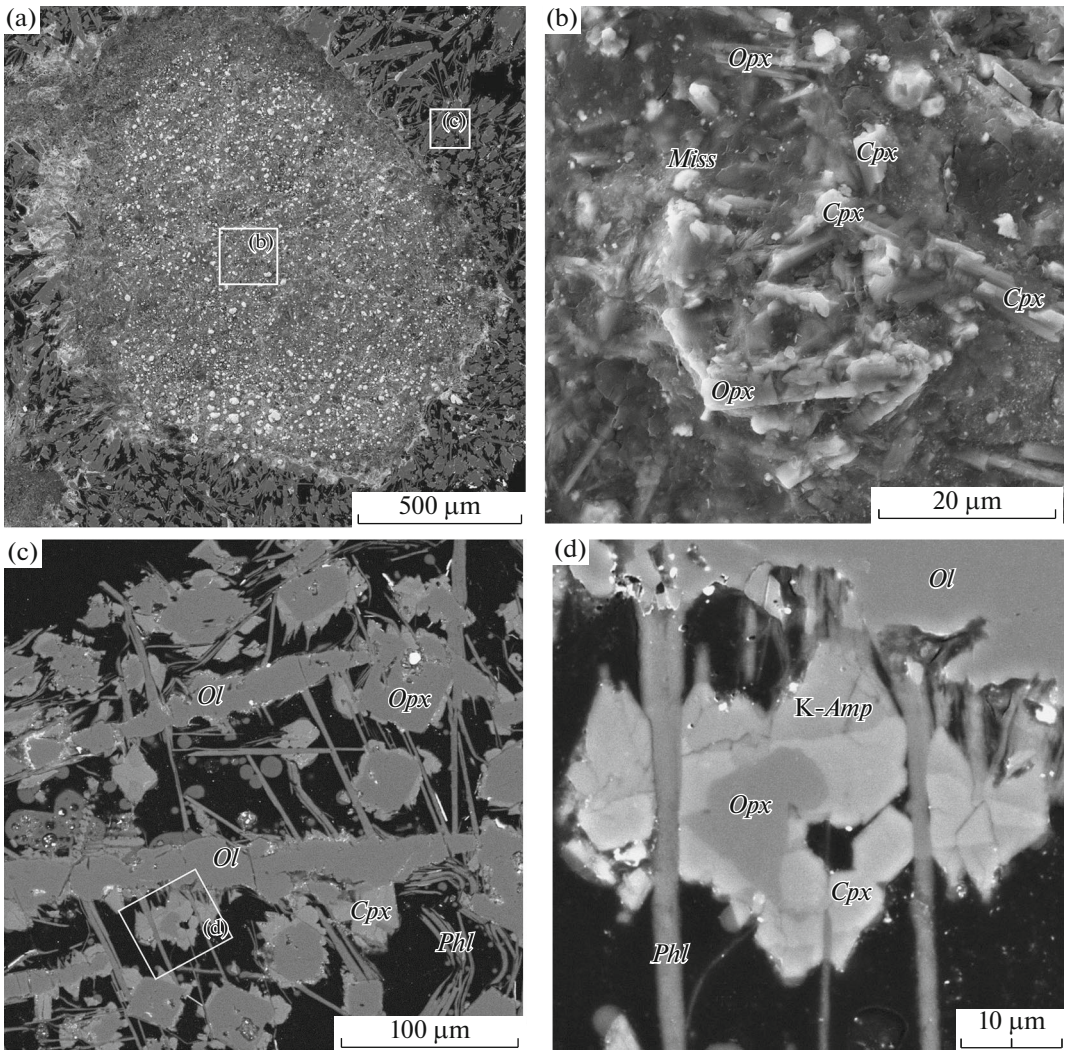

Fig. 7. BSE images of experimental samples in the peridotite–basalt–$(K,Na)_2CO_3$–H_2O system at 1400°C and 4.0 GPa. (a) Longwise section of sample capsule, peridotite–basalt contact; (b) basaltic part of sample represented by finely dispersed mixture of quenched silicate phases; (c) peridotite part of the sample; residual olivine (*Ol*), orthopyroxene (*Opx*), clinopyroxene (*Cpx*) in association with newly formed clinopyroxene (*Cpx*), phlogopite (*Phl*), K-amphibole (K-*Amp*), carbonate (*Cb*), and globules of quench glass (L_{Sil}); (d) magnified area in Fig. (c), reaction relations of orthopyroxene (*Opx*) ← clinopyroxene (*Cpx*) ← K-amphibole (K-*Amp*).

clinopyroxene ← K-bearing amphibole; among other phases are quench phlogopite (*Phl*) and carbonate (*Cb*), as well as globules of aluminosilicate glass (*Gl*).

DISCUSSION

Peridotite–H_2O System

Run products in the peridotite–H_2O system are characterized by the anomalous structure and phase composition. Their main peculiarity is the absence of intergranular glass, which caused the disintegration of samples. The absence of evidence for partial melting cannot be explained by the fact that experimental temperature was less than solidus temperature, because the solidus of water-saturated peridotite depending on its composition within 3–6 GPa varies from 800–820 to 1000–1100°C (Till et al., 2012). The similarity of structure and phase composition of samples within the range of 1000–1300°C gives grounds to suggest that the temperature of all these experiments (not only at $T \geq 1100$°C) corresponded to supersolidus conditions.

It was previously shown (Gorbachev, 2000; Gorbachev et al., 2015) that the transition of the silicate–fluid system from subcritical to supercritical state is clearly seen from the comparison of structure and phase composition of samples obtained in experiments in the silicate–fluid system of the same composition using the same technique at different (subcritical and supercritical) pressures and temperatures.

Regardless of experimental technique, samples obtained by partial melting in dry and hydrous conditions are characterized by monolithic texture, where silicate glass cements residual silicate and oxide phases. Quench phases in the glass and globules of immiscible sulfide or carbonate melts do not change the monolithic texture of the sample. The anomalous structure and phase composition of quench samples within 1000–1300°C can be explained by the existence of critical relations between silicate melt formed by partial melting of peridotite and aqueous fluid. The supercritical liquid dissolved peridotite minerals, and reaction garnet–clinopyroxene rims were formed around relicts of olivine–orthopyroxene peridotite.

In experiments at 1000 and 1100°C, olivine is characterized by high Th, U, Nb, Ta, Zr, and REE contents, which exceed those in garnet, clinopyroxene, and orthopyroxene. This means that the trace-element partition coefficients between olivine and supercritical fluid melt are higher than between garnet, clinopyroxene, orthopyroxene and supercritical fluid melt (L): $D^{Ol/L} > D^{(Grt,Cpx,Opx)/L}$. Partial melting of peridotite at subcritical pressures show opposite relations: $D^{Ol/L} < D^{(Grt,Cpx,Opx)/L}$. The absence of such enrichment in higher temperature (1200 and 1300°C) samples indicates that only near-solidus supercritical liquids are enriched in trace elements and have high dissolving and reaction ability, causing trace elements enrichment in olivine.

Available experimental data make it possible to estimate the minimum pressure of the formation of supercritical liquids during partial melting of hydrous peridotite. Some works (Till et al., 2012; Green et al., 2010; Grove et al., 2006; Kawamoto and Holloway, 1997; Kushiro, 1968; Mysen and Boettcher, 1975) revealed the absence of critical relations between melts and aqueous fluid at $P \le 3.0$ GPa. With allowance for experimental data by (Gorbachev, 1989, 2000; Gorbachev et al., 2015), this indicates that at partial melting of hydrous peridotite, supercritical liquids exist at $P \ge 3.8$ GPa within 1000–1300°C. The dissolution of peridotite minerals and formation of reaction "breccias" of garnet–clinopyroxene composition with relicts of olivine and orthopyroxene were caused by the interaction of supercritical fluid melts with residual minerals, while isolated microglobules of silicate glass are the quench products of this fluid melt.

Figure 8 shows the stability diagram of *Fo*, *En*, and *Pyr* versus $\log a(SiO_2)$ and $\log a(Al_2O_3)$ in supercritical liquid. This diagram was plotted using the concept of thermodynamic systems with perfectly mobile components and rules of constructing the multisystems with inert and perfectly mobile components (Korzhinskii et al., 1973; Zharikov, 1978). In the SiO_2–Al_2O_3–MgO system, at inert behavior of MgO and perfectly mobile behavior of SiO_2 and Al_2O_3, the chemical potential of which is given by supercritical liquid, the interaction of the latter with peridotite is simulated by the following monovariant reactions:

$$(Mg_2SiO_4)_{Ol} + (SiO_2)_L = 2(MgSiO_3)_{Opx}, \quad (1)$$

$$3(MgSiO_3)_{Opx} + (Al_2O_3)_L = (Mg_3Al_2Si_3O_{12})_{Grt}, \quad (2)$$

$$3(Mg_2SiO_4)_{Ol} + 2(Al_2O_3)_L + 3(SiO_2)_L = 2(Mg_3Al_2Si_3O_{12})_{Grt}. \quad (3)$$

In the diagram (Fig. 8), the coordinates of ternary point *Fo* + *En* + *Pyr* are determined by equations (1) and (2), while an equation of monovariant line is determined by the following reaction:

$$(Mg_2SiO_4)_{Ol} + (MgSiO_3)_{Opx} + (Al_2O_3)_L + (SiO_2)_L = (Mg_3Al_2Si_3O_{12})_{Grt}. \quad (4)$$

Using thermodynamic data (Nicholls et al., 1971; Nicholls and Carmichael, 1972; Robie and Hemingway, 1995) on temperature and pressure dependence $\log K = \Delta G(T, P)/2.3RT$ for reactions (1) and (2), the coordinates of ternary point *Fo* + *En* + *Pyr* at $T = 1500$ K, $P = 4$ GPa can be calculated as follows: $\log a(SiO_2)_L = -1.13$ and $\log a(Al_2O_3)_L = -0.49$. For true compositions of minerals, these values of $a(SiO_2)_L$ and $a(Al_2O_3)_L$ will be true for equilibria (1) and (2) at ratios of component activities in the right-hand (reaction products) and left-hand (starting phases) sides equal 1.

Experimental results indicate that asthenospheric lenses could exist in the upper mantle fluid-bearing peridotite at supersolidus temperatures and pressures ≥3.8 GPa. These lenses represent partial melting regions of peridotite with supercritical liquids enriched in incompatible elements. They are geochemically similar to undepleted mantle. At shallower depths, peridotites shall contain subcritical intergranular melts depleted in trace elements. The existence of such zoning will affect the geochemical features of basaltic magmas generated from peridotites (Fig. 9). Judging from the composition of mid-ocean ridge (MOR) basalts generated at depths less than critical pressure, melting of their sources under subcritical conditions does not lead to the enrichment in incompatible elements. Mantle reservoirs with supercritical intergranular liquid could serve as a source of incompatible element-rich ocean island basalts and riftogenic subalkaline basalts of trap provinces.

The vertical and lateral zoning of the Siberian superplume can explain the geochemical features of lavas of the Permian–Triassic trap province of the Siberian Platform. The activation of the Permian–Triassic (250 Ma) tectonomagmatic activity at the Siberian Platform under the influence of the Siberian superplume is ascribed to the global-scale catastrophic magmatic manifestations. It spanned an area of 1.5 million km^2, while the volume of magmatic products (lava, tuffs, intrusions) is more than 1 million km^3 (Masaitis, 1983). The trap magmatism began and

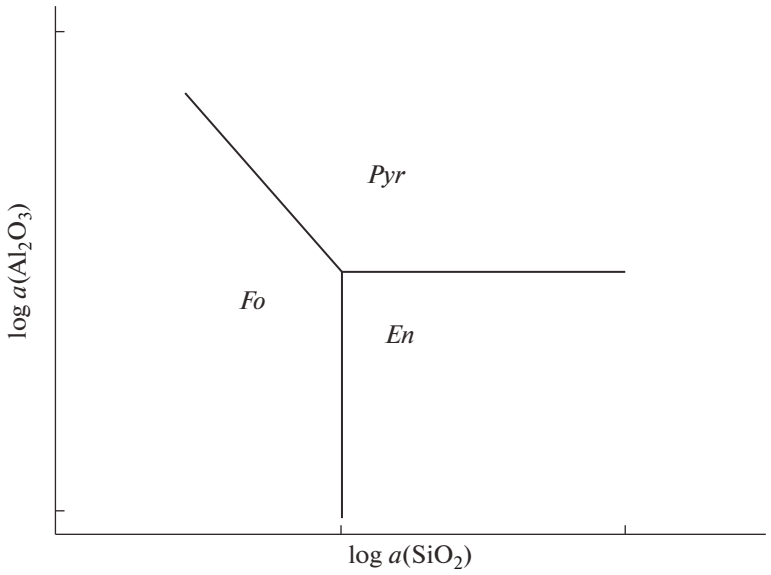

Fig. 8. Dependence of association forsterite (*Fo*)–enstatite (*En*)–pyrope (*Pyr*) on the log$a(SiO_2)$ and log$a(Al_2O_3)$ of supercritical liquid.

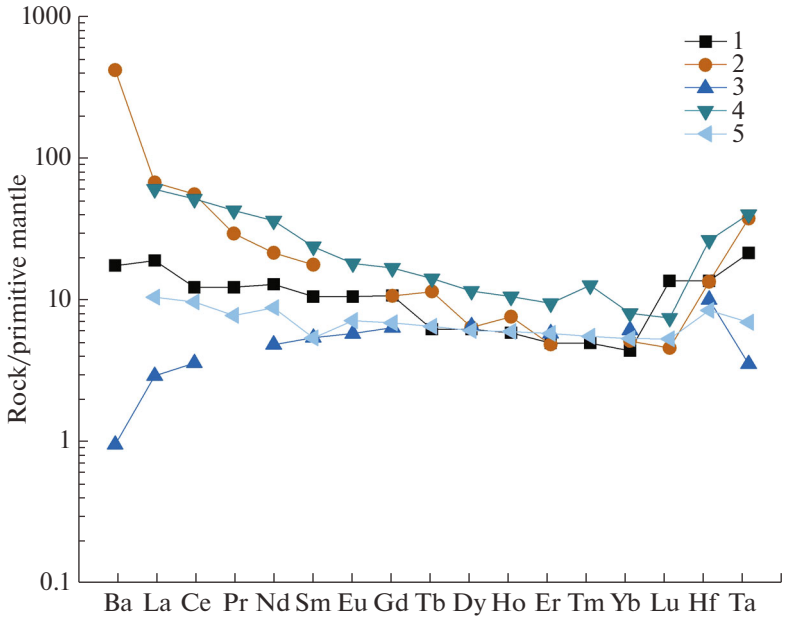

Fig. 9. Primitive mantle normalized trace element content in the basaltic series of different geodynamic settings. (1) Ocean islands, (2) continental within-plate settings (Kovalenko et al., 2007), (3) mid-ocean ridges (Bogatikov et al., 2010), (4, 5) traps of the Siberian platform: (4) Ivakinskaya Formation, (5) Mokulaevskaya Formation (Lightfoot et al., 1990).

reached peak intensity at the northwestern margin of the platform, in the Norilsk district (Gorbachev, 2010). A volcanogenic tuff–lava sequence 3.5 km thick, 45 thou km^2 in area, and 152 thou km^3 in volume was formed in this area (Fedorenko, 1981). Its lower horizons represented by the rift-related Ivakinskaya, Syverminskaya, and Gudzikhinskaya formations are developed only within the Norilsk district. The lavas are represented by high-Ti basalts enriched in incompatible elements. Geochemically, they are similar to ocean-island basalts (Lightfoot et al., 1990), which testifies to an enriched plume source with intergranular supercritical liquids. With ascent and propagation of plume head in a diffuse spreading setting, volcanism was developed over the entire area of the trap province (Putorana Plateau and Tungusskaya

syneclise). These conditions provided the generation of low-Ti MOR basalts. Their formation depths corresponded to subcritical pressures.

Supercritical liquids caused secondary enrichment, "refertilization" of depleted harzburgite or dunite residuals with trace and incompatible elements ("cryptic" metasomatism), and the replacement of olivine–orthopyroxene association by newly formed garnet and clinopyroxene ("modal" metasomatism). Disintegration of fluid-bearing mantle peridotite protolith at supercritical pressures could lead to the formation of tectonically weakened zones, which served as fluid pathways.

Basalt–H_2O System

In the **basalt**–H_2O system, the solidus and liquids temperatures are more than 1000°C and 1300°C, respectively. The Na_2O-rich (up to 6 wt %) silicate melts of trachybasaltic composition were formed within the entire temperature interval. The disintegrated texture of sample and the absence of silicate glass at 1000°C and 3.7 GPa indicate critical relations between melt and aqueous fluid. This results in the formation of supercritical highly reactive alkaline liquid, which caused the enrichment of garnet in titanium, the replacement of garnet by clinopyroxene, and the formation of ilmenite. The residue has a garnetite composition. The supercritical liquid interacts with the garnet crystals to cause a local melting with formation of alkali melt, which formed a glass at the contact with garnet during quenching. With increase of temperature from 1100°C to 1300°C and pressure from 3.8 to 4 GPa, the critical relations are absent, while eclogite experienced partial melting with formation of Na-alkaline silicate melt coexisting with garnetite at 1100°C. At 1150°C and 1300°C, garnet disappears, while Na-alkaline silicate melt coexists with clinopyroxene.

Thus, partial melting of hydrous basalt leads to the formation of supercritical liquid at 1000°C and 3.7 GPa. This process results in the formation of garnet with elevated (>10 mol %) content of schorlomite end-member $Ca_3Ti_2(Si,Fe)_3O_{12}$ corresponding to isomorphism $2Al + Si \leftarrow 2Ti + Fe$. A transition of eclogite into garnetite observed in the experiments during partial melting of the basalt–H_2O system at upper mantle *P-T* conditions indicates the possible formation of garnetites in the upper mantle through the interaction of subcritical and supercritical hydrous melts with residual minerals. The experiments demonstrate that the upper mantle garnetites differ from garnetites of the mantle transition zone, where eclogite to garnetite transition is related to increasing solubility of clinopyroxene component in garnet with formation of majorite garnet through isomorphic replacement $2Al \leftarrow Mg + Si$ (Collerson et al., 2000; Collerson et al., 2010; Gasparik, 1989). The comparison of garnets from experiments in the basalt–H_2O system at 3.7–3.9 GPa and 1000–1100°C and garnets from the transition zone at 12 GPa and 900°C (Okamoto and Maruyama, 2004) shows that the garnets from the transition zone as compared to the upper mantle garnets are enriched in Si, Ti, Ca, depleted in Al, Fe, and have similar proportions of Mg and Na.

Peridotite–Basalt–$(K,Na)_2CO_3$-H_2O System

At experimental *P-T* conditions, critical relations were reached between carbonated silicate melt and fluid. This follows from structural features and phase composition of samples: the disintegration of peridotite capsule and the absence of intergranular silicate glass in it. After experiment, the peridotite capsule filled with a mixture of basalt and carbonates consisted of a pressed mixture of micron-sized silicate and carbonate particles, which were formed at quenching of supercritical liquid. Reaction relations in residue with replacements of olivine←orthopyroxene←clinopyroxene←potassium-bearing amphibole-type are caused by the interaction of peridotite with supercritical liquid. The wide development of reaction relations among residual peridotite minerals indicates the high chemical activity of the latter. The composition of supercritical liquid is characterized by the presence of phlogopite and globules of aluminosilicate glass and carbonate. Melting of supercritical mantle reservoir with subducted oceanic protolith at pressures and temperatures exceeding critical values should be accompanied by decompaction of the protolith owing to peridotite disintegration.

The structural features and phase composition of samples under supercritical conditions suggest a zoned structure of reservoirs with subducted oceanic protoliths: the outer zone represented by disintegrated harzburgite or dunite residue, which was metasomatically altered by supercritical liquid and experienced "refertilization" owing to the formation of new minerals, and the inner zone consisting of isolated lenses of supercritical liquid.

CONCLUSIONS

At supercritical *P-T* parameters, the regions of partial melting (asthenospheric lenses) exist in the fluid-bearing upper mantle. They contain near-solidus incompatible elements-enriched supercritical liquids, which possess high extracting and reactive ability. Mantle reservoirs with supercritical liquids are geochemically similar to enriched mantle and could serve as a source of incompatible element-enriched ocean-island basalts and riftogenic subalkaline basalts of trap provinces. Disintegration of fluid-bearing mantle peridotite protolith at supercritical pressures could lead to the formation of tectonically weakened zones, which served as pathways for fluids and upper mantle plumes.

The modal and cryptic metasomatism of the upper mantle under the influence of supercritical liquids leads to the refertilization of depleted harzburgite or dunite residue, with enrichment of residual minerals in trace and incompatible elements, replacement of peridotite olivine–orthopyroxene assemblage by newly formed garnet–clinopyroxene one. Eclogitization of peridotite during interaction with supercritical liquids could serve as an efficient mechanism of overcoming the "eclogite" barrier. This effect could also explain also the coexistence of peridotite and eclogite mineral assemblages in mantle xenoliths and inclusions in diamonds (Wang, 1998; Sobolev, 1974). The interaction of subcritical and supercritical fluid-bearing melts with residual minerals at partial melting of eclogites provides the eclogite to garnetite transition at upper mantle *P-T* conditions.

FUNDING

This work was carried out at the Institute of Experimental Mineralogy of the Russian Academy of Sciences in the framework of the State Task (project no. AAAA-A18-118020590140) and was partially supported by the Russian Foundation for Basic Research (project no. 17-05-00930a).

CONFLICT OF INTEREST

The authors declare that they have no conflict of interest.

REFERENCES

Bogatikov O.A., Kovalenko V.I., Sharkov E.V. *Magmatizm, tektonika, geodinamika Zemli* (Magmatism, Tectonics, and Geodynamics of the Earth), Moscow: Nauka, 2010.

Bureau, H. and Keppler, H., Complete miscibility between silicate melts and hydrous fluids in the upper mantle: experimental evidence and geochemical implications, *Earth Planet. Sci. Lett.,* 1999, vol. 165, pp. 187–196.

Collerson, K.D., Hapugoda, S., Kamber, B.S., and Williams, Q., Rocks from the mantle transition zone: majorite-bearing xenoliths from Malaita, southwest Pacific, *Science,* 2000, vol. 288, pp. 1215–1223.

Collerson, K.D., Williams, Q., Kamber, B.S., et al., Majoritic garnet: a new approach to pressure estimation of shock events in meteorites and the encapsulation of sub-lithospheric inclusions in diamond, *Geochim. Cosmochim. Acta,* 2010, vol. 74, pp. 5939–5957.

Fedorenko, V.A., Petrochemcial series of volcanic rocks of the Norilsk district, *Geol. Geofiz.,* 1981, no. 6, pp. 78–88.

Gasparik, T., Transformation of enstatite–diopside–jadeite pyroxenes to garnet, *Contrib. Mineral. Petrol.,* 1989, vol. 102, pp. 389–405.

Gorbachev, N.S., *Flyuidno-magmaticheskoe vzaimodeistvie v sul'fidno-silikatnykh sistemakh* (Fluid-Magmatic Interaction in Sulfide–Silicate Systems), Moscow: Nauka, 1989.

Gorbachev, N.S., Supercritical state in the hydrous mantle: evidence from experimental study of fluid-bearing peridotite at $P = 40$ kbar and $T = 1400$°C, *Dokl. Earth Sci.,* 2000, vol. 370, no. 1, pp. 147–149.

Gorbachev, N.S. Experimental study of interaction between fluid-bearing basaltic melts and peridotite: a mantle–crustal source of trap magmas in the Norilsk Area, *Petrology,* 2010, vol. 18, no. 4, pp. 416–431.

Gorbachev, N.S., Kostyuk, A.V., and Shapovalov, Yu.B., Experimental study of the peridotite–H_2O system at $P = 3.8$–4 GPa and $T = 1000$–1400°C: critical relations and vertical zoning of the upper mantle, *Dokl. Earth Sci.*, 2015, vol. 461, no. 4, 360–363.

Green, D.H., Hibberson, W.O., Kovacs, I., and Rosenthal, A., Water and its influence on the lithosphere–asthenosphere boundary, *Nature,* 2010, no. 7314, pp. 448–451.

Gregoire, M., Moine, B.N., Oreiliy, S.Y., et al., Trace element residence and partitioning in mantle xenoliths metasomatized by highly alkaline, silicate-and carbonate-rich melts (Kerguelen Islands, Indian Ocean), *J. Petrol.,* 2000, vol. 41, no. 4, pp. 477–509.

Grove, T.L., Chatterjee, N., Parman, S.W., and Medard, E., The influence of H_2O on mantle wedge melting, *Earth Planet. Sci. Lett.,* 2006, vol. 249, no. 1–2, pp. 74–89.

Kawamoto, T. and Holloway, J.R., Melting temperature and partial melt chemistry of H_2O-saturated mantle peridotite to 11 gigapascals, *Science,* 1997, vol. 276, no. 5310, pp. 240–243.

Keppler, H. and Audetat, A., Fluid–mineral interaction at high pressure. Mineral behavior at extreme conditions, *EMU Notes Mineral.,* 2005, vol. 7, pp. 225–251.

Kessel, R., Ulmer, P., Pettke, T., et al., The water-basalt system at 4 to 6 GPa: phase relations and second critical endpoint in a K-free eclogite at 700 to 1400°C, *Earth Planet. Sci. Lett.,* 2005, vol. 237, pp. 873–892.

Klein-BenDavid, O., Izraeli, E.S., Hauri, E., and Navon, O., Fluid inclusions in diamonds from the Diavik Mine, Canada and the evolution of diamond-forming fluids, *Geochim. Cosmochim. Acta,* 2007, vol. 71, pp. 723–744.

Korzhinskii, D.S., *Teoreticheskie osnovy analiza paragenezisov mineralov* (Theoretical Principles of Analysis of Mineral Parageneses), Moscow: Nauka, 1973.

Kovalenko V.I., Naumov V.B., Girnis A.V., et al., Average compositions of magmas and mantle sources of mid-ocean ridges and intraplate oceanic and continental settings estimated from the data on melt inclusions and quenched glasses of basalts, *Petrology,* 2007, vol. 15, no. 4, pp. 335–368.

Kushiro, I., Compositions of magmas formed by partial zone melting of the Earth's upper mantle, *J. Geophys. Res.,* 1968, vol. 73, pp. 619–634.

Lightfoot, P.C., Naldrett, A.J., Gorbachev, N.S., et al., Geochemistry of the Siberian trap of the Noril'sk area, USSR, with implication for the relative contributions of crust and mantle to flood basalt magmatism, *Contrib. Mineral. Petrol.,* 1990, vol. 104, no. 3, pp. 631–644.

Litasov, K.D. and Ohtani, E., Effect of mater on the phase relations in Earth's mantle and deep water cycle, *Sp. Pap. Geol. Soc. Am.,* 2007, vol. 421, pp. 115–156.

Litvin, Yu.A., *Fiziko-khimicheskie issledovaniya plavleniya glubinnogo veshchestva Zemli* (Physicochemical Studies of Deep Earth Melting), Moscow: Nauka, 1991

Mallik, A. and Dasgupta, R., Reaction between MORB-eclogite derived melts and fertile peridotite and generation of ocean island basalts, *Earth Planet. Sci. Lett.,* 2012, vol. 329–330, pp. 97–108.

Masaitis, V.L., Permian and Triassic magmatism of Siberia: problems of dynamic reconstructions, Zap. Vsesoyuz. Mineral. *O-va*, 1983, vol. 4, pp. 412–425.

Mibe, K., Kanzaki, M., Kawamoto, T., et al., Second critical endpoint in the peridotite–H_2O system, *J. Geophys. Res.,* 2007, vol. 112, p. B03201.

Mysen, B. and Boettcher, A.L., Melting of a hydrous mantle: parts I and II. Phase relations of a natural peridotite at high pressures and temperatures with controlled activities of water, carbon dioxide, and hydrogen, *J. Petrol.,* 1975, vol. 16, no. 3, pp. 520–593.

Navon, O., Hutcheon, I.D., Rossman, G.R., and Wasserburg, G.J., Mantle-derived fluids in diamond microinclusions, *Nature,* 1988, vol. 335, pp. 784–789.

Nicholls, J. and Carmichael, I.S.E., The equilibration temperature and pressure of various lava types with spinel- and garnet peridotite, *Am. Mineral.,* 1972, vol. 57, pp. 941–959.

Nicholls, J., Carmichael, I.S.E., and Stormer, J.C., Jr. Silica activity and P_{total} in igneous rocks, *Contrib. Mineral. Petrol.,* 1971, vol. 33, pp. 1–20.

Okamoto, K. and Maruyama, Sh., The eclogite–garnetite transformation in the MORB + H_2O system, *Phys. Earth Planet. Int.,* 2004, vol. 146, pp. 283–296.

Ringwood, A.E. and Green, D.H., An experimental investigation of the gabbro–eclogite transformation and some geophysical implications, *Tectonophysics,* 1966, vol. 3, pp. 383–427.

Robie, R.A. and Hemingway, B.S., Thermodynamic properties of minerals and related substances at 298.15 K and 1 bar (105 pascals) pressures and at higher temperatures, *US Geol. Survey Bull,* 1995, no. 2131.

Sobolev, N.V., *Glubinnye vklyucheniya v kimberlitakh i problemy sostava verkhnei mantii* (Deep-Seated Inclusions in Kimberlites and Problem of Upper Mantle Composition), Novosibirsk: Nauka, 1974.

Stalder, R., Ulmer, P., Thompson, A.B., and Gunther, D., High pressure fluids in the system $MgO–SiO_2–H_2O$ under upper mantle conditions, *Contrib. Mineral. Petrol.,* 2001, vol. 140, pp. 607–618.

Taylor, L.A. and Neal, C.R., Eclogites with oceanic crustal and mantle signatures from the Bellsbank kimberlite, South Africa, Part 1: mineralogy, petrography, and whole rock chemistry, *J. Geol.,* 1989, vol. 97, pp. 551–567.

Till, C.B., Grove, T.L., and Withers, A.C., The beginnings of hydrous mantle wedge melting, *Contrib. Mineral. Petrol.,* 2012, vol. 163, pp. 669–688.

Tumiati, S., Fumagalli, P., Tiraboschi, C., and Poli, S., An experimental study on COH-bearing peridotite up to 3.2 GPa and implications for crust–mantle recycling, *J. Petrol.,* 2013, vol. 54, pp. 453–479.

Wang, W., Formation of diamond with mineral inclusions of "mixed" eclogite and peridotite paragenesis, *Earth Planet. Sci. Lett.,* 1998, vol. 160, no. 3, pp. 831–843.

Weiss, Y., Kessel, R., Griffin, W.L., et al., A new model for the evolution of diamond-forming fluids: evidence from microinclusion-bearing diamonds from Kankan, Guinea, *Lithos,* 2009, vol. 112, no. 2, pp. 660–674.

Wyllie, P.J. and Ryabchikov, I.D., Volatile components, magmas, and critical fluids in upwelling mantle, *J. Petrol.,* 2000, vol. 41, pp. 1195–1206.

Yaxley, G.M., Experimental study of the phase and melting relations of homogeneous basalt plus peridotite mixtures and implications for the petrogenesis of flood basalts, *Contrib. Mineral. Petrol.,* 2000, vol. 139, pp. 326–338.

Zharikov, V.A., *Osnovy fiziko-khimicheskoi petrologii* (Principles of Physicochemical Petrology), Moscow: MGU, 1978.

Translated by M. Bogina